ESA Contract Report

ESA 4000130590/20/NL/IA

Contract Report to the European Space Agency

WP-3000 Developing a flexible system to simulate and assimilate small satellite data

Technical Note 3 (final version) for ESA contract no. 4000130590/20/NL/IA

Authors: Katie Lean, Niels Bormann and Sean Healy

December 2021

Series: ECMWF ESA Contract Report Series

A full list of ECMWF Publications can be found on our web site under:
http://www.ecmwf.int/en/publications/

Contact: library@ecmwf.int

European Centre for Medium Range Weather Forecasts, Shinfield Park, Reading, RG2 9AX, UK

Contents

Abstract

In preparation for running Ensemble of Data Assimilations (EDA) experiments for testing the impact of constellations of small satellites carrying microwave (MW) sounders, a flexible system to simulate and assimilate the small satellite data has been implemented. External orbital parameter files are received and re-formatted for use in the ECMWF assimilation system. High resolution model fields produced using the latest operational version of the system are used in combination with a radiative transfer model and the sampling provided through the external files to calculate the simulated brightness temperatures (BTs) for the small satellites. A thinning procedure is applied to the data and perturbations related to the instrument noise are added to the simulated observations. Finally, assimilation tests show that the data can be used to actively influence the assimilation system. While the underpinning technical work is complete, adjustments should be considered in particular to tune the perturbations to achieve realistic simulated BTs.

1 Introduction

Small satellites are expected to become an important component of the future global observing system used for Numerical Weather Prediction (NWP), complementing a continuing core constellation of larger platforms. Constellations of small satellites would be able to provide a cost-effective option to greatly increase the temporal sampling. In this project we are investigating the optimal design for a future constellation of small satellites carrying microwave (MW) sounding instruments. A selection of 10 different potential constellations will be chosen to particularly examine the relative benefits of:

- Increasing the number of satellites and varying the type of orbit, potentially combining polar and low inclination orbits
- The use of humidity sensitive channels only (around 183GHz), which are more easily accommodated on smaller, lighter instruments, or having additional temperature sounding capabilities (around 50GHz)

The evaluation of the impact of each scenario will be conducted using the Ensemble of Data Assimilations (EDA) method. The EDA consists of multiple cycling assimilation systems where each member is generated through perturbations to the observations, model physics and boundary conditions (Isaksen et al., 2010). Simulated small satellite data and the associated observation errors for each constellation will be added to a consistent baseline of existing observations representing a possible future situation of reduced numbers of the current, more advanced MW sounding instruments. For this baseline, only four satellites corresponding to two in each of the current Metop and JPSS orbits (local equator crossing times of 09:30 and 01:30 respectively) will be included to provide existing MW sounding observations. The benefit of additional simulated data from each constellation is measured by the reduction in the variation across the members (known as the ensemble spread) which equates to improving the forecast or analysis uncertainties. The final list of scenarios is still under discussion but expected to be confirmed in the near future.

Previous work packages covered preparatory work informing the future EDA experimentation. This included establishing four weeks as the length of EDA experiment needed to achieve robust statistics (Lean et al., 2021a). The study period has thus been chosen to cover 1-28 June 2018 which also coincides with the analysis period used by Duncan and Bormann (2020) to show the continued benefit from adding existing MW sounding data. The results from Duncan and Bormann (2020) provide a valuable reference with use of the existing data before we extend to future constellations and allowed investigation of the relationship between EDA spread changes and forecast error statistic changes measured by

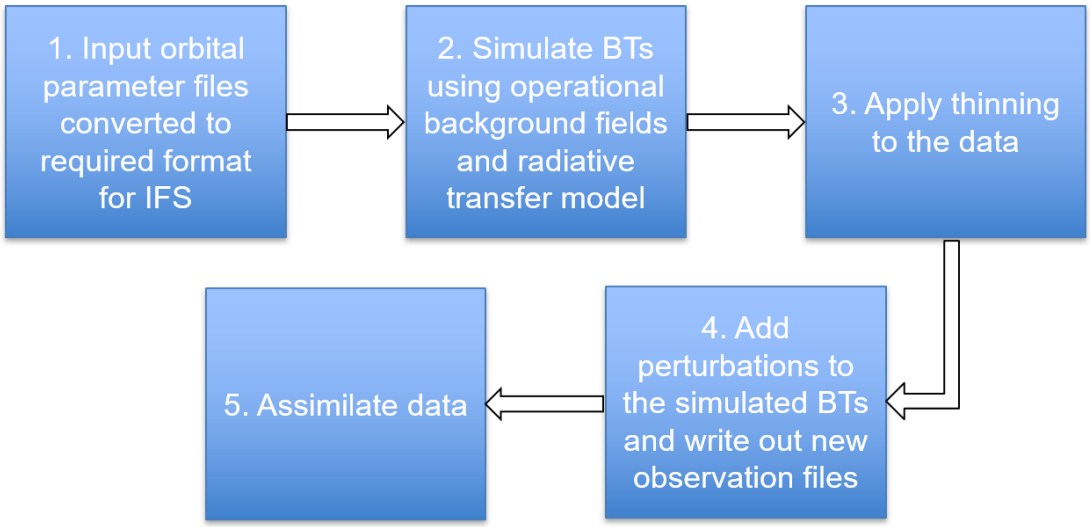

Figure 1: Flowchart to illustrate the steps to producing simulated small satellite data ready to assimilate in the ECMWF system, starting from receipt of externally produced input parameter files. The Integrated Forecast System (IFS) is the ECMWF atmospheric model and data assimilation system. BT = Brightness Temperatures.

traditional Observing System Experiments (OSEs) (Lean et al., 2021b). While there was no one-to-one correspondence, it was shown that the EDA spread changes are qualitatively consistent with forecast error reductions seen in OSEs. Further activities included adaptation of the observation error model to account for the unavailability of key lower frequency channels on the small satellites.

This third phase of the project focuses on the technical set up needed for running the EDA experiments. Here we have designed a flexible system to simulate and assimilate the small satellite constellation data. This work is carried out with input from a partner ESA project (comprising collaboration with JCR Systems Ltd, Informus GmbH, In-Space Systems and Fluctus SAS) whose work includes providing the orbital parameter input files i.e. the locations in space and time of the data to be simulated and instrument noise estimates.

Orbital parameter input data for a constellation using Arctic Weather Satellite (AWS) based instruments have been provided by the partner project. In this scenario, there are eight satellites across four orbital planes with two satellites at 180° apart in each plane. The local equator crossing times for the four planes are 05:30 07:30, 11:30 and 15:30. This provides equally distributed orbits in time when accounting for the presence of MW sounders on the larger platform satellites in the Metop and JPSS orbits used in the proposed baseline observing system used for the experiments. The scenario provided has been used for development and testing of the system to simulate and assimilate the new observations.

In the following, we give a brief overview of the system development, summarising each stage of the processing. Conclusions and a look ahead to the next phase are given in section 3. Different stages of processing are illustrated with the AWS-based, eight satellite constellation. The emphasis is on demonstrating the technical capabilities, whereas some design-choices will be refined subsequently.

2 Data processing overview

In work package 3000, the technical framework has been developed to generate and assimilate the observations from a constellation of small satellites within ECMWFs Integrated Forecast System (IFS). Figure 1 outlines the processing steps required, starting from the constellation data provided by the partner project. In the following, we describe each step and summarise key design choices. The system has been designed to allow full flexibility in the geographical/temporal sampling available from the constellation of small satellites. Spectral characteristics of the channels to be simulated follow the Microwave Sounder (MWS) on Metop-SG.

2.1 Converting orbital parameter files to format required by IFS

The first step of the processing consists of converting the constellation sampling files provided to a format that can be read by the IFS. These orbital files are received in NetCDF format and contain the spatial and temporal information for the satellite observations throughout the four week experiment period (1st -28th June 2018) split into six hour chunks for each satellite. Variables provided in the files are:

- Latitude and longitude of observation
- Satellite zenith and azimuth angles for each observation
- Time of observation (given in days after 00Z 1 Jan 2000)
- Latitude and longitude of subsatellite point
- Altitude of satellite

Following an AWS-based design, there are 113 fields of view across each scan and a maximum scan angle of 54.41°.

Satellite data used at ECMWF are usually received in Binary Universal Form for the Representation of meteorological data (BUFR) and converted to Observation DataBase (ODB) format, developed at ECMWF, which is used within the assimilation system. An alternative route therefore had to be developed to ingest the sampling information to the IFS. This uses the so-called "Experimental Observations Framework" developed for ingesting new data that is not available in standard BUFR files and converting it to the expected ODB format. It relies on a specific data-layout in NetCDF, and then allows new data to be incorporated alongside existing observations in the assimilation system.

A module (written in Python coding language) has been developed which reads in the originally provided NetCDF files and creates the required new structure. This also sets other auxiliary parameters, such as sensor or satellite identifiers which are needed in the IFS to distinguish different datasets. A new NetCDF file is produced for each six hour chunk for each satellite. For the Experimental Observations Framework to process the data into the ODB structure, an accompanying file for the whole dataset is also provided with acts as a translation from the NetCDF file to the ODB variable names. Figure 2 shows the sub satellite point for one six hour period with each satellite track given in a different colour according to the unique identifier assigned for use in the assimilation system.

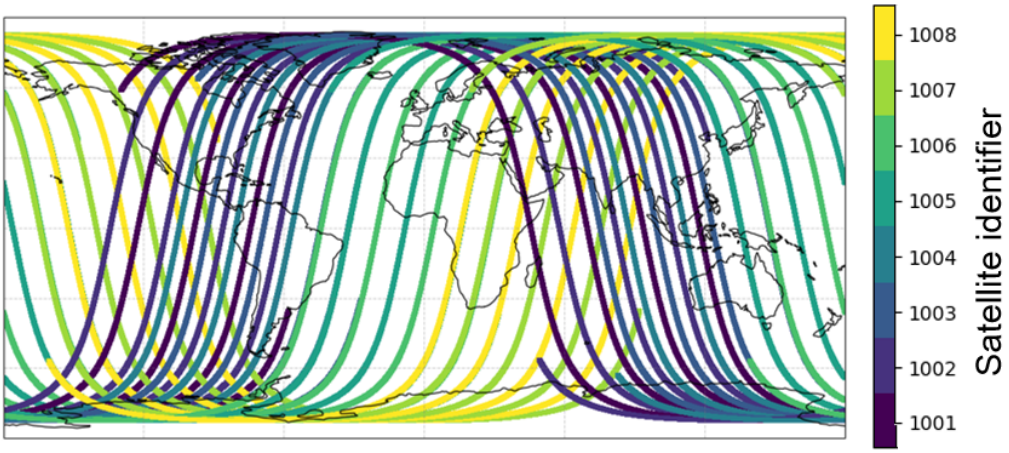

Figure 2: Ground track for 8 satellites in AWS-based constellation for a six hour period centred on 00Z 2nd June 2018. Different colours denote the unique satellite identifier number assigned to each satellite for use during assimilation.

2.2 Producing simulated brightness temperatures

The brightness temperatures for the small satellite data are simulated from high-resolution ECMWF fields, using a tailored configuration of the IFS. To achieve this, the IFS has been modified to process data from the new sensor on-board the small satellites. The spectral channel characteristics are modelled on MWS, and the processing replicates as far as possible that of the all-sky assimilation of existing MW sounding data (Geer et al., 2014; Duncan et al., 2021). As in the operational ECMWF 4D-Var assimilation system, the processing is done in 12-hour windows. Within these 12-hour windows, we use the forecast model combined with a radiative transfer model to provide physically consistent values of model equivalents at the observation locations in space and time. The process replicates that used during the assimilation of real MW observations. Observations can either be simulated from the background trajectory (i.e. a short-range forecast) or an analysis trajectory (i.e. the result of assimilating all other observations during the 12-hour window).

2.2.1 High-resolution model fields

The model fields used for the simulation have been produced at the operational resolution $T_{Co}1279$ ($\sim$9km) with 137 vertical levels. Cycle 47R1.4 of the Integrated Forecast System (IFS) is used, which is the operational configuration at the time of this work. For the period in question, the ECMWF analyses benefit from the assimilation of five MW humidity sounding and six MW imaging instruments in the all sky framework and eight MW temperature sounders in the clear-sky framework. Additionally, three hyperspectral infrared instruments from platforms in the Metop and JPSS orbits are assimilated as well as other significant observing system components including radio occultation, atmospheric motion vectors and conventional observations such as radiosondes and aircraft.

2.2.2 *Radiative transfer model*

The radiative transfer model used is RTTOV-SCATT[1] which accounts for scattering from hydrometeors at MW frequencies and therefore allows use of the MW data in the all sky framework (Saunders et al., 2020). We make use of version 13 of RTTOV-SCATT which benefits from a comprehensive update in the description of frozen hydrometeors (Geer, 2021) and other developments. For producing the simulated observations here and later during assimilation, we use coefficients generated for MWS. The small satellites across all the proposed scenarios will be using a sub-selection of channels available on MWS. The input to RTTOV-SCATT consists of a model profile interpolated to the geo-location provided in the constellation sampling file, taking the slanted viewing geometry into account (Bormann, 2017). The spatial extent of the satellite footprint is not explicitly modelled.

Over the ocean, surface emissivity is calculated for both existing or simulated MW data using the Fast Microwave Ocean Emissivity Model (FASTEM version 6) which does not rely on the observed BTs (Kazumori and English, 2015). However, surface emissivity over non-ocean surfaces is treated slightly differently for the small satellite data compared to approaches used for real MW data. In the assimilation of real MW sounding data, a retrieval of emissivity is performed using the observed BT from the 50.3GHz channel for the temperature sounding and using either the 90 or 150GHz channels for the humidity sounding (Karbou et al., 2006; Baordo and Geer, 2016). This is because an adequate surface emissivity model is presently not available for the required frequencies. As we are simulating the small satellite data at this stage, we cannot follow this dynamic retrieval method for the emissivity. Instead, values will be provided by an emissivity atlas over snow-free land surfaces (Aires et al., 2011) or estimated values over more difficult snow and sea ice surfaces. While the atlas emissivity is considered a fully adequate replacement over snow-free land surfaces, the emissivity specification over snow and sea-ice surfaces is relatively crude and it will not capture the full variability and complexity of the emissivity variations over these regions.

Surface emissivity for snow-covered land and sea-ice areas are treated as follows: if the model surface skin temperature is less than 278K, or the model sea-ice fraction is greater than zero, the emissivity is calculated using fractions of different surface types (open ocean, sea ice and land) as given by the model fields. These are used as weights with corresponding emissivity values to provide the final emissivity estimate (equation 1) where the FASTEM value is used over ocean surface and constant values of 0.8 and 0.95 are used over sea ice (with any degree of snow cover) and snow covered land respectively.

$$emis\_backup = frac\_ocean * fastem\_emis + frac\_seaice * 0.8 + frac\_land * 0.95 \quad (1)$$

In the above equation, $frac\_ocean$, $frac\_seaice$ and $frac\_land$ are the fractions of the scene made up of open ocean, sea ice and land respectively while $fastem\_emis$ is the emissivity provided by the FASTEM calculations (pers. comm. A. Geer, July 2021). This means in practice that all scenes comprising sea ice only would receive an emissivity value of 0.8 while for purely land scenes where the possibility of snow is detected, the emissivity will be 0.95. Over snow, we use a constant value for all frequencies, even though snow emissivity can vary significantly depending on the conditions of the snow-pack, both temporally and spectrally. With further advances in snow emissivity modelling, the aim would be to eventually replace this simple framework with more sophisticated models. However, it is beyond the scope of this project to develop such improvements. As the study period is June, the impact of using this simple model particularly for snow covered land should be minimised for the Northern Hemisphere.

Note that in the later assimilation step, the dynamic retrieval can be employed again as the simulated

[1] RTTOV = Radiative Transfer for TOVS, TOVS = TIROS Operational Vertical Sounder, TIROS = Television Infrared Observation Satellite

BTs will be present in the required window channels. The retrieved emissivities for the small-satellite data will then not be consistent with those from other MW sounders, but since there is no interaction between different emissivity retrievals in the IFS this is not considered a major problem. However, no attempt is made at modelling biases related to biases in the effective model skin temperature which can be considerable over snow and sea-ice. As a result of these approximations, the simulation of the impact of the small-satellite data over snow and sea-ice surfaces is hence likely to be optimistic.

2.2.3 Calculating small satellite simulated brightness temperatures

In order to take advantage of the latest developments in treatment of MW data, the simulated brightness temperatures will be generated using a version of the IFS based on cycle 47R3.0 (which became the operational configuration on 12 Oct 2021) but with an added package of improvements to the MW processing. This set of MW changes has been undergoing rigorous testing and is submitted for the next model upgrade, cycle 48R1. The same IFS package (47R3.0 plus MW improvements) will be used later for the assimilation in the EDA experiments. Note that in cycle 47R3 the assimilation of AMSU-A observations has been extended from clear-sky-only to all-sky assimilation (Duncan et al., 2021). The advancements in the treatment of MW data for cycle 48R1 include the move to v13 of the RTTOV radiative transfer model, and a significant increase of the use of surface-sensitive MW radiances over land or sea-ice surfaces, primarily for MW imager observations.

The output of the simulation are BTs for all MWS channels, available in ODB format. At this stage in the processing, no error sources have been included in the BT simulation. These are added in a later step (see 2.4). Figure 3 shows the simulated BTs using the small satellite configuration alongside the bias corrected real BTs from the equivalent channel on the Metop-B AMSU-A/MHS instruments. The similar atmospheric structures and overall good agreement support the method of simulation. Figure 4 illustrates the simulated BTs for a single channel across all eight satellites.

2.3 Offline thinning

Prior to the assimilation of any MW sounding data at ECMWF, the observations are thinned in space and time. This is to mitigate against the presence of spatially correlated observation errors, primarily arising from representation errors (e.g., radiative transfer errors, errors due to differences in the spatial scales that are represented). It is currently technically not possible to account for such spatial observation error correlations during the assimilation, and the applied thinning mitigates against overfitting the assimilated data.

For the all-sky assimilation of real MW sounding data, thinning is carried out during an initial pre-processing stage of screening that occurs while the data are still in the originally received BUFR format. An equivalent thinning process for the simulated small satellite data has been written using a combination of Fortran and Python programmes. The input to this thinning module is the full dataset of simulated observations from the previously described step in ODB format. The thinning is based on selecting, within a specified time-slot, the observation closest to a reduced Gaussian grid point. This ensures an even geographic sampling. The length of the time-slot and the resolution of the Gaussian grid can be chosen freely by the user.

When constructing this new code, in practice, there are two steps performed:

1. Each satellite is treated separately and for each time-slot only the closest observation to each grid

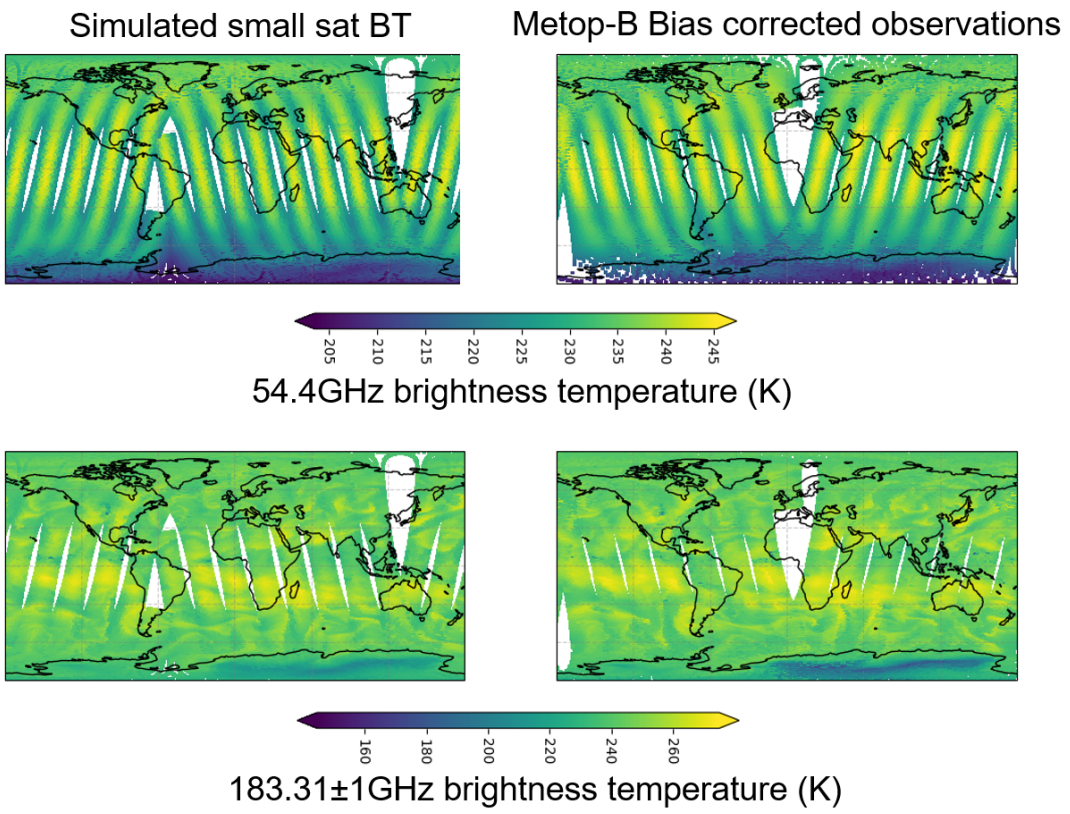

Figure 3: Simulated brightness temperatures (left) for the AWS-based constellation compared to equivalent bias corrected observations (right) from Metop-B AMSU-A and MHS. The tropospheric temperature sounding channel at 54.4GHz (top) and humidity sounding channel at 183.31±1GHz (bottom) illustrate the realistic values and structures seen across all the channels in the simulated data. Data are for one 12-hour cycle on 2 June 2018.

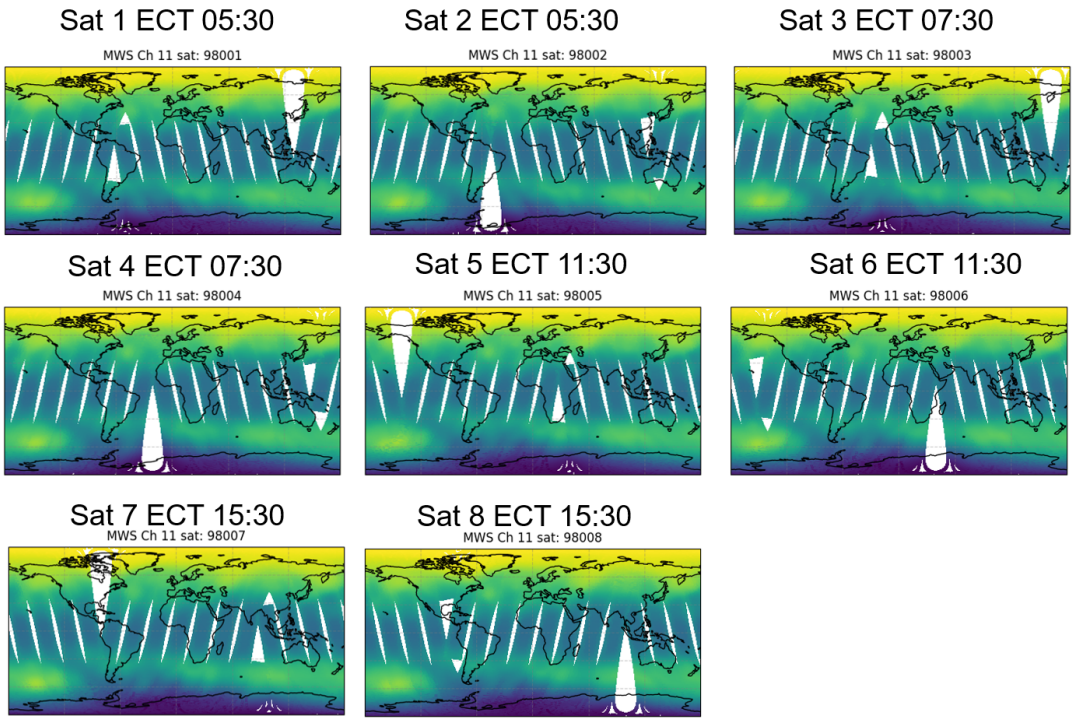

Figure 4: Simulated 57.290GHz brightness temperatures for all eight satellites in the AWS-based constellation for the 12 hour assimilation window of 00Z 2 June 2018. This is a temperature sounding channel equivalent to AMSU-A 9 which has peak sensitivity around 90hPa.

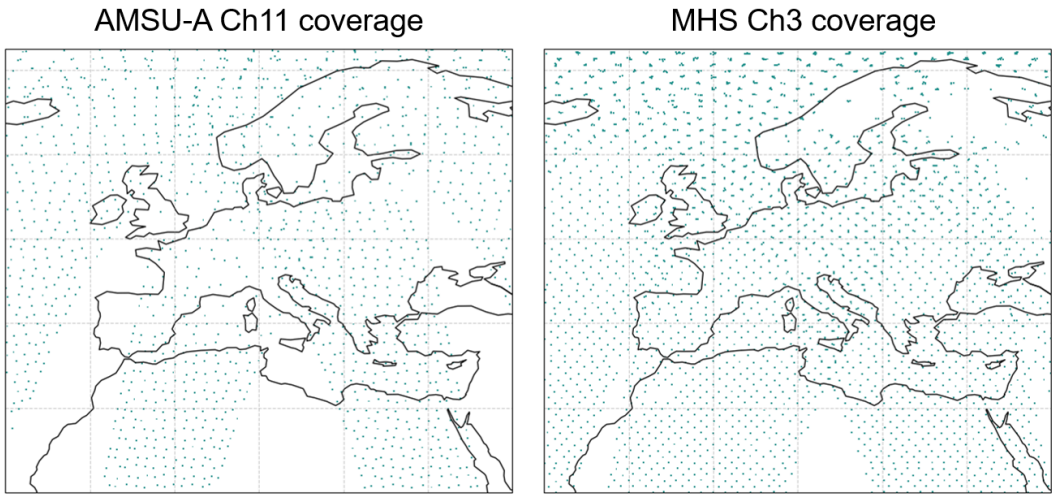

Figure 5: Data density resulting from the different thinning strategies for temperature and humidity sounding instruments in the all sky framework illustrated by the actively assimilated data from Metop-B AMSU-A 11 (left) and MHS 3 (right) for one 12 hour cycle at 12Z 20 Oct 2021.

point for each satellite is retained.

2. All the satellites in the constellation pre-thinned from step 1 are then thinned together to again find the observation closest to each grid point from all the small satellites. This facilitates combined thinning of several satellites in a constellation.

Step one is comparatively far slower than step two. Splitting the process into the two parts anticipates the repetitive use of same orbit across multiple constellations. Therefore when the same orbit is present in another constellation scenario, processing to this point will not need to be repeated for this satellite, including the earlier initial BT simulation detailed in section 2.2.

For operational MW sounding data, slightly different thinning scales are used in the IFS for the humidity and temperature sounding instruments in the all sky framework. For temperature-sounding observations, a reduced Gaussian grid of T_L159 is used, hence resulting in a minimum-separation distance of around 125 km. For humidity-sounding instruments, a reduced Gaussian grid of T_L255 is used, but data for only every 2nd Gaussian grid-point are retained, with the selection alternating in the meridional direction. This results in a minimum separation distance between observations of around 110 km. While the choices result in slightly denser coverage for humidity-sounders, the two thinning methods do not produce particularly different outcomes in the density (figure 5). For the small-satellite data, the same thinning scale will be employed for humidity and temperature sounding channels. Given the relatively small differences in the thinning scales, the effect of choosing one over the other is expected to be relatively small, and the denser option (T_L255 grid, alternate grid points) will be used. In line with the assimilation of AMSU-A, the time-slot will be set to 30 min, and observations from all satellites of the small-satellite constellation will be thinned together. That is, only data from one location will be selected per Gaussian grid point, within a half-hour interval.

This part of the processing involves a large reduction in observation numbers, for example for one satellite in the AWS-based constellation there were initially 140685 simulated observations for one channel

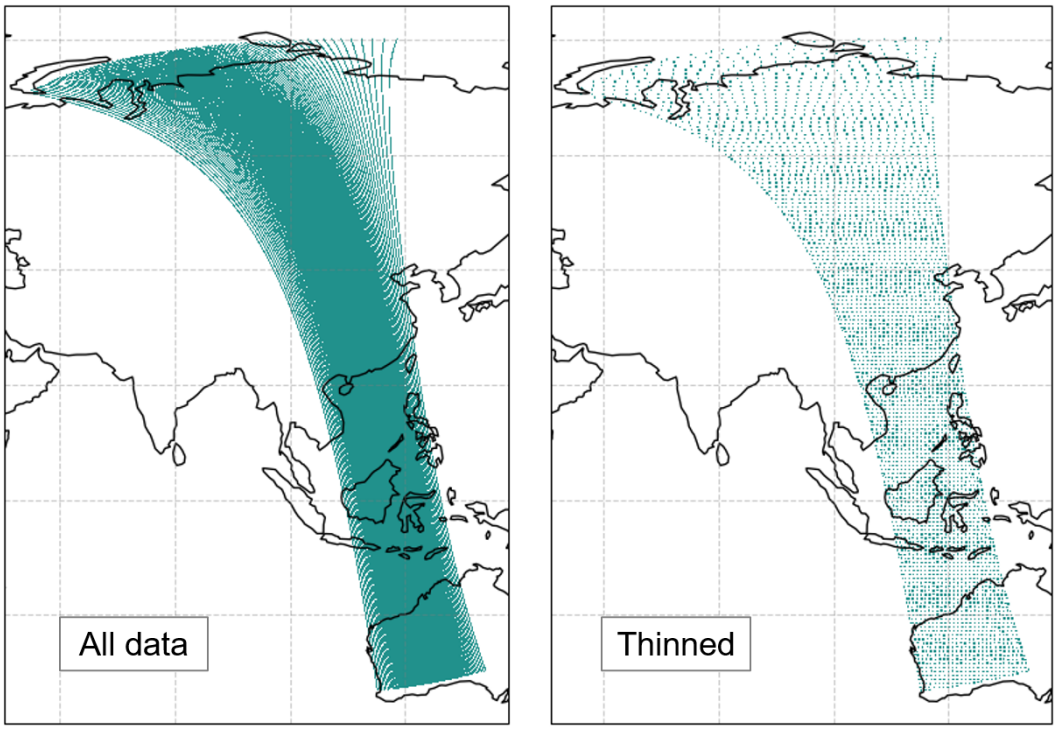

Figure 6: Location of observations for a single satellite before any thinning has taken place (left) and after the satellite has passed through thinning on its own. Data are for a 30 minute period 21:30–22:00Z 2 June 2018.

during a 30 minute period (21:30-22:00Z, 2 June 2018). Figure 6 illustrates how this reduces to 4457 observations for one channel after individual thinning in step one above. There is a further reduction to 4155 following thinning with the other seven satellites. Figure 7 shows the coverage for all eight satellites after being thinned together.

2.4 Adding noise to simulated observations

Prior to assimilating in the EDA, perturbations must be added to the simulated observations to simulate instrument noise and potentially other error sources. For each observation, a random number is drawn from a Gaussian distribution with mean of zero and standard deviation of one. This is multiplied by the estimate of Noise Equivalent Differential Temperature (NEDT) (to be provided by the partner ESA project) of the associated channel on the instrument to generate the final perturbation. Therefore, channels with higher noise estimates such as the humidity sounding channels generally have perturbations larger in magnitude than those of the lower noise temperature sounding channels as demonstrated in figure 8. In this case, the clear sky observation error estimates from equivalent AMSU-A and MHS channels have been used as a substitute for technical development and illustrative purposes.

In addition to the perturbations that have been explicitly added, variability will also be introduced through the differences in resolution and IFS versions used during the simulation and assimilation. We would ideally like to replicate a similar distribution of differences in simulated observations and short-range

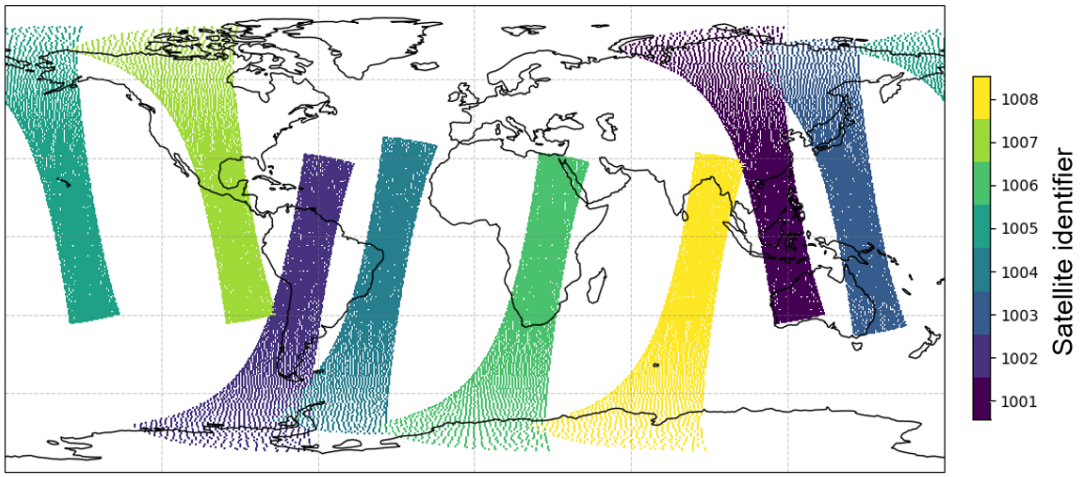

Figure 7: Coverage of all eight satellites after the offline thinning procedure has been carried out. Data are for a 30 minute period 21:30-22:00Z 2 June 2018.

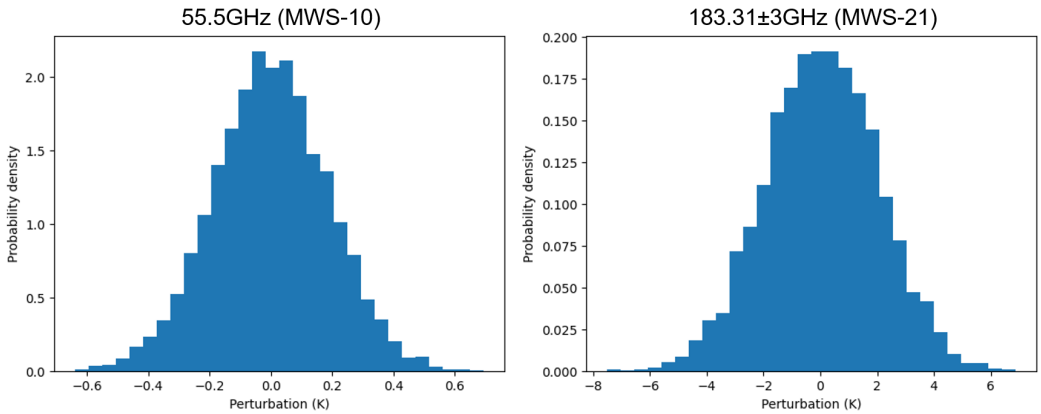

Figure 8: Histogram showing examples of variation in magnitude of the perturbations added to the simulated data prior to assimilation in the EDA for a low noise temperature channel peaking in the upper troposphere (left) and a higher noise humidity sounding channel (right) for observations for one satellite during one hour period.

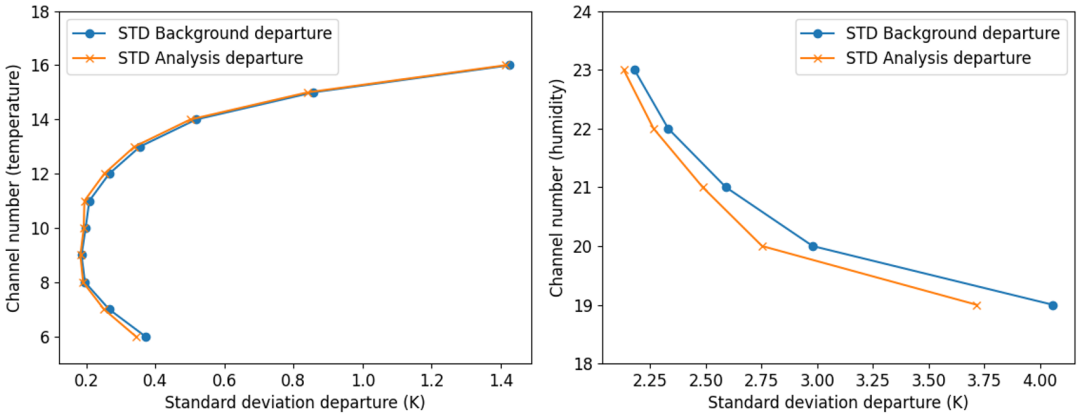

Figure 9: Standard deviation of background departure (blue) and analysis departure (orange) for temperature sounding channels around 53-57GHz (left) and humidity sounding channels around 183GHz (right). Data are from all eight satellites assimilated during one 12-hour cycle 00Z 2 June 2018.

forecast (known as background departure statistics) that we would typically find with real observations. However, it is not currently known exactly how important it is to achieve realistic departure statistics or the impact of the degree of realism. With the foundation of technical work now complete, longer assimilation periods of the data with the noise estimates (to be provided by the ESA partner project) allow an investigation of the background departures from the simulated observations.

It should be noted here that these noise-affected simulated observations are further perturbed in the EDA, with different perturbations in each EDA member to sample the uncertainty in the observations. These perturbations in the EDA will be consistent with the observation error model used in the assimilation. It is expected that the perturbations added in the EDA are the main factor affecting the spread of the EDA. If necessary, the basis for these initial perturbations can be tuned accordingly. Note that the NEDT values will also be important in the construction of the observation error calculation. For now, temporary values are used for input to the observation error model for the small satellites in the next assimilation step.

2.5 Assimilation

After completing the steps outlined so far, simulated BTs have been produced, thinned and perturbed and are now ready for assimilation. Rather than immediately test with EDA experiments which are expensive, tests have been run using a deterministic assimilation system traditionally used for research assimilation experiments of real data. Channels on the small satellite follow the same processing as equivalent channels on e.g. AMSU-A/MHS. As shown in figure 9 the assimilation successfully draws to the simulated data, as is evident from smaller standard deviations of analysis departures compared to background departures. These profiles show only the active data (i.e. contributing to cost function computed throughout the assimilation processing) which includes all the thinning steps and quality control, for example some channels with surface sensitivity are rejected over snow/ice regions.

The current simulation of the new observations does not include the addition of any systematic errors, arising, for instance from errors in the calibration or the radiative transfer. Such biases are removed as part of the assimilation through variational bias correction (VarBC) (Auligné et al., 2007), and including such biases in the generation of the simulated data is hence not considered essential. However, it is

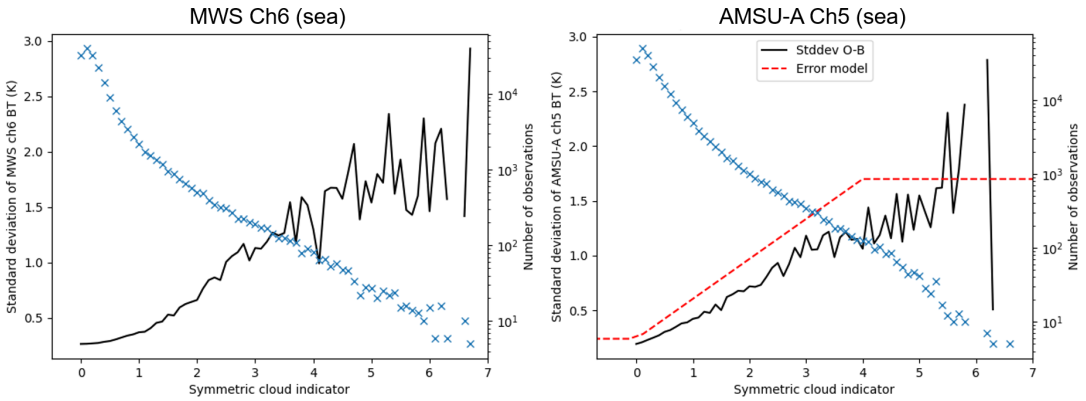

Figure 10: Standard deviation of observation - background departures for all eight small satellites MWS ch6 (left) and Metop-C AMSU-A ch5 (right) - which is a low peaking tropospheric sounding channel - binned as a function of symmetric cloud predictor using AMSU-A channel 4 or equivalent for MWS. The symmetric cloud indicator is an average of model and observation contributions. Crosses indicate the number of observations in each bin. Data are over ocean only from 00Z 2 June 2018 (MWS) and 1 -10 Dec 2020 (AMSU-A), limited to ±60N to exclude sea ice contamination and are actively used observations taken from an experiment assimilating AMSU-A and MWS in an all-sky framework.

important to avoid that the assimilation system treats the simulated observations as anchor observations, i.e. observations that are assimilated without bias correction and hence inform the bias correction of other observations. Therefore, we nevertheless activate the use of VarBC for the observations from small satellites, allowing for a separate bias correction for each instrument and channel consistent with the treatment of all other sounding data. The handling of biases in the small-satellite observations is a limitation in our current approach and could be revisited in future work. Nevertheless, the approach is equivalent to assuming that in the mean over all instruments the bias in the new satellite constellation is small, a situation that is broadly consistent with the experience from existing sensors. It is also worth noting that in any case the EDA is designed to estimate random forecast errors, and the influence of systematic errors in the EDA is a subject of ongoing research.

At present, noise levels in the small satellite data are likely to be higher in general compared to equivalent real observations due to the use of clear sky values in the perturbation generation rather than the estimated NEDT values. In assessing the realism of the simulated data, figure 10 and 11 consider the dependence of the standard deviation of background departures on an indicator of cloud which forms the basis of the all sky observation error model. For reference, figure 8 from the WP-2000 report where the observation error model is discussed in more detail (Lean et al., 2021b), has been reproduced here as well to allow easier comparison with real observations from AMSU-A for the equivalent channel. A brief outline of the all sky observation error model has also been added for reference in Appendix A. The standard deviation (and correspondingly the eventual assigned observation error) should increase in the presence of cloud in either the model or observations. As required, there is a similar dependence where the standard deviation of the background departures using the simulated small satellite data increases as a greater presence of cloud is indicated for both temperature and humidity sounding channels. This suggests that the simulated data do contain some realistic structures and cloud features in the background departure statistics.

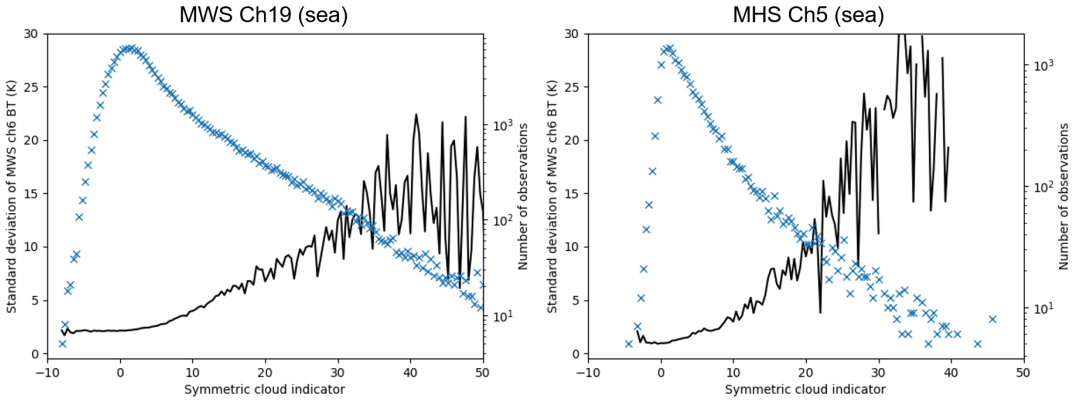

Figure 11: Standard deviation of observation - background departures for all eight small satellites MWS ch19 (left) and Metop-B MHS ch5 (right) - which is the lowest peaking humidity sounding channel - binned as a function of symmetric cloud predictor. The symmetric cloud indicator is an average of model and observation contributions. Crosses indicate the number of observations in each bin. Data are over ocean only from 00Z 2 June 2018, limited to $\pm$60N to exclude sea ice contamination and are actively used observations taken from an experiment assimilating MHS and MWS in an all-sky framework.

3 Summary

In this technical phase, a flexible system has been designed for the processing of small satellite data from receipt of external orbital parameter files to the final simulated BTs being successfully assimilated. BTs are simulated from high resolution model fields using a radiative transfer model. The data are then thinned and perturbations added that currently follow random noise controlled by the NEDT values of each instrument channel. Finally, the data are assimilated, following the all-sky assimilation approach developed at ECMWF for cross-track scanning MW temperature and humidity sounders.

The system is flexible to be able to process satellites in different orbital planes and combinations and with different channel subsets available. With the underpinning technical work complete the next step is to refine the treatment of observational uncertainties in the generation of the simulated data:

- Situation-dependence of representation error is currently not included in the perturbations applied. However, the standard deviation of the observed - background BTs for the simulated data already displays key features of departure statistics for real data, for example in the dependence on the indicator of cloud. A longer assimilation period would help to confirm these results but initial findings here suggest that treatment of representation error relating to clouds may already be adequate. It is also worth noting that it is likely that the perturbations added within the EDA remain the determining factor and that the results may be insensitive to minor deviations from true observations.
- Observational biases are currently ignored when the observations are simulated. However, VarBC nevertheless needs to be activated in the assimilation, as the simulated observations will otherwise be inappropriately used as anchor observations. The behaviour of the resulting bias correction will need to be monitored in longer assimilation trials.

Looking ahead to running EDA experiments, the final list of scenarios to be tested will soon be decided.

The partner ESA project, in addition to the input orbital parameters, is also advising on possible constellations that span a range of complexity. This will allow us to choose a sub-selection that can answer questions on the optimum number and orbit of the satellites and the trade-off between humidity only or with additional temperature sounding capabilities. Where there are satellite orbits in common across the different constellations, some of the steps described in the report will not need to be repeated. For example, for two constellations where the only difference is the subset of channels (e.g. humidity only or humidity plus temperature sounding) the active channels can be controlled through an auxiliary input file. Therefore, the processing steps only need to be completed fully once and for the second experiment and it is then possible to go straight to the final active assimilation.

Acknowledgements

The authors would like to thank Alan Geer and David Duncan for providing valuable discussion and technical support, in particular the provision of the IFS code branch containing recent MW improvements submitted for later operational use and on the process of calculating MW emissivity.

Appendix A Outline of the all sky observation error model

The observation error for MW sounding observations typically comprises of measurement error, such as originating from instrument noise, the forward model error, e.g. from the radiative transfer calculations, and representation error, arising from different scales and processes being represented in the observations and the model fields. In the case of all-sky use, the representation error dominates the observation error in cloudy conditions, arising from different representativeness of clouds in the observations and the model fields. This is accounted for by an observation error model that assigns larger observation errors in cloudy regions, based on a suitable indicator of the presence of clouds in the observations or the model fields (Geer and Bauer, 2011). Figure 12 shows a simple schematic of the formulation in terms of the cloud indicator.

The all-sky observation error is applied to a selection of temperature and humidity sounding with sensitivity to the presence of clouds. Where temperature sounding channels have a peak sensitivity in the stratosphere, the impact of cloud is negligible so the error model becomes a constant value. For MW temperature sounding channels, different cloud indicators are used for AMSU-A data and the simulated small satellite data due to the availability, or not, of lower frequency channels. For AMSU-A, there are two different cloud indicators used in the error model corresponding to land or ocean surfaces. Over land, the difference 23.8-89GHz provides a scattering index which exploits the increased scattering from frozen hydrometeors at 89GHz compared to 23.8GHz (Bennartz et al., 2002). Over ocean, the indicator is the retrieved liquid water path (Grody et al., 2001) which is derived from 23.8GHz and 31.4GHz channels. For the small satellite data, an indicator based on the 52.8GHz channel which measures the cloud effect in a window channel will be used over both land and sea (Lean et al., 2021b). Meanwhile, for humidity sounding channels around 183GHz, a scattering index utilises channels at 89GHz and 150GHz (Geer et al., 2014) (which both remain available in the small satellite configuration). Differences in scattering from precipitation-sized ice particles are exploited, similar to the land scattering index model for AMSU-A temperature sounding channels.

The cloud indicator used in the error model is formulated by taking the average of the cloud indicator

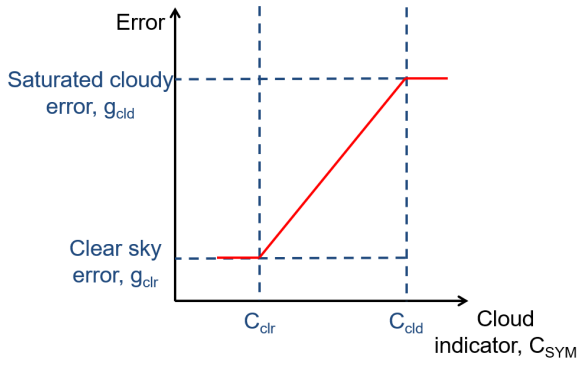

Figure 12: Simple schematic showing how the coefficients in equations 3 - 5 define the form of the error model.

values for the observations and the model background:

$$C_{SYM} = (P_{obs} + P_{bkrd})/2 \tag{2}$$

Where P_{obs} is the indicator calculated using observed values e.g. the difference in observed brightness temperatures at 23.8 and 89 GHz for the scattering index and P_{bkrd} is calculated using the model background equivalent brightness temperatures. The final observation error is then constructed with either a linear or quadratic dependence on the cloud indicator as the following (reproduced in the linear form using the same notation from Geer et al. (2014)):

$$g_{clr} \in C_{SYM} <= C_{clr} \tag{3}$$

$$g(C_{SYM}) = g_{clr} + (g_{cld} - g_{clr}) \left(\frac{C_{SYM} - C_{clr}}{C_{cld} - C_{clr}} \right) \in C_{clr} < C_{SYM} < C_{cld} \tag{4}$$

$$g_{cld} \in C_{SYM} >= C_{cld} \tag{5}$$

Where g_{clr} and g_{cld} are the clear sky and saturated cloudy error values respectively while C_{clr} and C_{cld} are threshold values of the symmetric cloud indicator to separate clear and saturated cloudy situations, respectively. The clear sky values reflect the individual channel noise estimates of the instrument, inflated in recognition of other error sources in this situation e.g. from forward modelling error. The cloudy saturation value and the choice of a linear or quadratic nature of the model are determined by analysing the standard deviation of background departures binned as a function of the symmetric cloud indicator. These values are determined separately for each satellite and individual instrument channels. Figure 12 illustrates how the coefficients define the construction of the error model.

References

Aires, F., Prigent, C., Bernardo, F., Jimnez, C., Saunders, R., Brunel, P., 2011. A tool to estimate land-surface emissivities at microwave frequencies (telsem) for use in numerical weather prediction. QJRMS 137 (656), 690–699.

Auligné, T., McNally, A. P., Dee, D. P., 2007. Adaptive bias correction for satellite data in a numerical weather prediction system. QJRMS 133 (624), 631–642.

Baordo, F., Geer, A., 2016. Assimilation of SSMIS humidity-sounding channels in all-sky conditions over land using a dynamic emissivity retrieval. Q.J.R.M.S., 2854–2866.

Bennartz, R., Thoss, A., Dybbroe, A., Michelson, D., 2002. Precipitation analysis using the Advanced Microwave Sounding Unit in support of nowcasting applications. Met. Apps, 177–189.

Bormann, N., 2017. Slant path radiative transfer for the assimilation of sounder radiances. Tellus A: Dynamic Meteorology and Oceanography 69 (1), 1272779.

Duncan, D. I., Bormann, N., 2020. On the Addition of Microwave Sounders and NWP Skill, Including Assessment of FY-3D Sounders. EUMETSAT/ECMWF Fellowship Programme Research Report No.55.

Duncan, D. I., Bormann, N., Geer, A. J., Weston, P., 2021. Assimilation of AMSU-A in All-sky Conditions. EUMETSAT/ECMWF Fellowship Programme Research Report No.57.

Geer, A., Baordo, F., Bormann, N., English, S., 2014. All-sky assimilation of microwave humidity sounders. ECMWF Technical Memorandum No. 741, 57pp.

Geer, A. J., 2021. Physical characteristics of frozen hydrometeors inferred with parameter estimation. Atmospheric Measurement Techniques 14 (8), 5369–5395.
URL https://amt.copernicus.org/articles/14/5369/2021/

Geer, A. J., Bauer, P., 2011. Observation errors in all-sky data assimilation. Q. J. R. Meteorol. Soc. 137, 2024–2037.

Grody, N., Zhao, J., Ferraro, R., Weng, F., , Boers, R., 2001. Determination of precipitable water and cloud liquid water over oceans from the NOAA 15 advanced microwave sounding unit. J. Geophys. Res., 29432953.

Isaksen, L., Bonavita, M., Buizza, R., Fisher, M., Haseler, J., Leutbecher, M., Raynaud, L., 12 2010. Ensemble of data assimilations at ECMWF, 45.
URL https://www.ecmwf.int/node/10125

Karbou, F., Gérard, E., Rabier, F., 2006. Microwave land emissivity and skin temperature for AMSU-A and -B assimilation over land. QJRMS 132, 2333–2355.

Kazumori, M., English, S. J., 2015. Use of the ocean surface wind direction signal in microwave radiance assimilation. QJRMS 141 (689), 13541375.
URL https://rmets.onlinelibrary.wiley.com/doi/abs/10.1002/qj.2445

Lean, K., Bormann, N., Healy, S., January 2021a. Technical Note 1 for ESA Contract No. ESA 4000130590/20/NL/IA: WP-1000 Review of EDA approach and recommendations for small satellite configurations. ESA Contract 4000130590/20/NL/IA Technical Note 1 (unpublished), ECMWF, Reading, UK.

Lean, K., Bormann, N., Healy, S., January 2021b. Technical Note 2 for ESA Contract No. ESA 4000130590/20/NL/IA: WP-2000 Calibration of EDA spread and adaptation of the observation error model. ESA Contract 4000130590/20/NL/IA Technical Note 2 (unpublished), ECMWF, Reading, UK.

Saunders, R., Hocking, J., Turner, E., Havemann, S., Geer, A., Lupu, C., Vidot, J., Chambon, P., K´opken-Watts, C., Scheck, L., Stiller, O., Stumpf, C., Borbas, E., 2020. RTTOV-13 science and validation report. EUMETSAT NWP SAF, version 1.0.
URL https://nwp-saf.eumetsat.int/site/software/rttov/documentation/